Title page

GPR139, an orphan receptor highly enriched in the habenula and septum, is activated by the essential amino acids L-tryptophan and L-phenylalanine

Changlu Liu, Pascal Bonaventure, Grace Lee, Diane Nepomuceno, Chester Kuei, Jiejun Wu, Qingqin Li, Victory Joseph, Steven W Sutton, William Eckert, Xiang Yao, Lynn Yieh, Curt Dvorak, Nicholas Carruthers, Heather Coate, Sujin Yun, Christine Dugovic, Anthony Harrington and Timothy W. Lovenberg

Janssen Research & Development, LLC. CL, PB, GL, DN, CK, JW, QL, VJ, SWS, WE, XY, LY, CD, NC, HC, SY, CD, AH, TWL

Running title page

a) Running title: GPR139 is activated by L-tryptophan and L-phenylalanine

b) Corresponding author: Pascal Bonaventure, Janssen R&D, LLC. 3210 Merryfield Row,

San Diego, CA 92121. Email: Pbonave1@ its.jnj.com; phone: 858-784-3078

c) The number of   Text pages: 54

Tables: 4

Figures: 8

References: 29

Words in the Abstract: 241

Words in the Introduction: 587

Words in the Discussion: 2105

d) List of nonstandard abbreviations: cAMP, cyclic adenosine monophosphate; CHO, Chinese hamster ovary cells; DMEM, Dulbecco's modified eagle medium; DMSO, dimethyl sulfoxide; EDTA, ethylenediaminetetraacetic acid; ERK, extracellular signal-regulated kinases; FBS, fetal bovine serum; FLIPR, fluorometric imaging plate reader; JNJ-63533054, [(S)-3-chloro-N-(2-oxo-2-((1-phenylethyl)amino)ethyl) benzamide]; FPKM, Fragments Per Kilobase per Million; JNJ-63770044, (R)-3-chloro-N-(2-oxo-2-((1-phenylethyl)amino)ethyl)benzamide)]; GTEx, Genotype-Tissue Expression; GTPγS, guanosine 5'-O-(3-thio)-triphosphate; HBSS, Hanks' balanced salt solution; HEK, human embryonic kidney; HEPES 4-(2-hydroxyethyl)-1-piperazineethanesulfonic acid; HPLC, high

performance liquid chromatography; LC/MS, liquid chromatography - mass spectrometry; LP-360924, (2-((4-methoxy-6-((3-methoxypropyl)amino)-1,3,5-triazin-2-yl)amino)-4-phenylthiazol-5-yl)(4-(pyrimidin-2-yl)piperazin-1-yl)methanone; LP-471756, 4-cyclohexyl-N-(o-tolyl)benzenesulfonamide; LP-114958, 3-benzyl-N,5-dicyclohexyl-3H-[1,2,3]triazolo[4,5-d]pyrimidin-7-amine); MAPK, mitogen-activated protein kinase; PAGE, polyacrylamide gel electrophoresis; PBS, phosphate buffered saline; PCPA, p-chlorophenylalanine; PCR, polymerase chain reaction; RACE, Rapid Amplification of cDNA Ends; SDS, sodium dodecyl sulfate; rpm, revolutions per minutes; PVDF, polyvinylidene difluoride; TCO-9311, (3,5-Dimethoxybenzoic acid 2-[(1-naphthalenylamino)carbonyl]hydrazide); TE, Tris EDTA buffer; Tris, 2-amino-2-hydroxymethylpropane-1,3-diol.

MOL#100412

Abstract

GPR139 is an orphan G-protein coupled receptor expressed in the central nervous system. To identify its physiological ligand, we measured GPR139 receptor activity from recombinant cells following treatment with amino acids, orphan ligands, serum and tissue extracts. GPR139 activity was measured using guanosine 5'-O-(3-[^{35}S]thio)-triphosphate binding, calcium mobilization and extracellular signal-regulated kinases phosphorylation assays. The amino acids, L-tryptophan (L-Trp) and L-phenylalanine (L-Phe) were found to activate GPR139, with EC$_{50}$ values in the 30-300 µM range, consistent with the physiological concentrations of L-Trp and L-Phe in tissues. Chromatography of rat brain, rat serum, and human serum extracts revealed two peaks of GPR139 activity which corresponded to the elution peaks of L-Trp and L-Phe. With the purpose of identifying novel tools to study GPR139 function, a high throughput screening campaign led to the identification of a selective small molecule agonist [JNJ-63533054, (*S*)-3-chloro-N-(2-oxo-2-((1-phenylethyl)amino)ethyl) benzamide]. The tritium-labelled JNJ-63533054 bound to cell membranes expressing GPR139 and could be specifically displaced by L-Trp and L-Phe. Sequence alignment revealed that GPR139 is highly conserved across species, and RNA sequencing studies of rat and human tissues indicated its exclusive expression in the brain and pituitary gland. Immunohistochemical analysis showed specific expression of the receptor in circumventricular regions of the habenula and septum in mice. Together, these findings suggest that L-Trp and L-Phe are candidate physiological ligands for GPR139, and we hypothesize that this receptor may act as a sensor to detect dynamic changes of L-Trp and L-Phe in the brain.

Introduction

The application of modern molecular biology techniques has led to the identification of 865 genes in the G-protein coupled receptor (GPCR) family (Fredriksson et al., 2003; Fredriksson and Schiöth, 2005). Activation of GPCRs can occur through binding of a variety of ligands including peptides, neurotransmitters, hormones, ions, light, pheromones, amino acids, amines, nucleosides and lipids. Given the importance of GPCRs in many aspects of physiology, they are among the most pursued targets for drug development (Heng et al., 2013; Lundstrom and Chiu, 2005; Overington et al., 2006). More than 30% of the drugs currently on the market target GPCRs; yet, to date, they only affect a small proportion of all known GPCRs. Thus, the potential for drug discovery within this field remains enormous. For this reason, orphan GPCRs represent an attractive source of new targets for drug discovery research. About 300 GPCRs were de-orphanized over the past two decades (Civelli et al., 2013). The rate of natural ligand discoveries has decreased, suggesting that the remaining orphan GPCRs may have non-classical ligands or ligands that are heretofore unanticipated by sequence homology analysis.

One such orphan, GPR139 (aka GPRg1 or GPCR12) was first identified as a Rhodopsin family GPCR with exclusive expression in the central nervous system (Gloriam et al., 2005; Matsuo et al., 2005). Its closest homologue, GPR142, however is expressed primarily in the pancreas and other peripheral tissues (Susens et al., 2006). *In situ* hybridization experiments in mouse brain showed that GPR139 mRNA is abundantly expressed in the septum, caudate, habenula, zona incerta and medial mammillary nucleus (Matsuo et al., 2005; Susens et al., 2006). The receptor has been reported to be coupled with Gq and constitutively active when

recombinantly expressed in mammalian cells (Matsuo et al., 2005). To date, three groups have reported surrogate small molecules for GPR139. Shi et al. identified a series of benzohydrazides as potent and selective surrogate agonists for GPR139, the most potent compound is also known as TCO-9311 (3,5-Dimethoxybenzoic acid 2-[(1-naphthalenylamino)carbonyl]hydrazide) (Shi et al., 2011). Hu et al. also identified surrogate agonists (including LP-360924, (2-((4-methoxy-6-((3-methoxypropyl)amino)-1,3,5-triazin-2-yl)amino)-4-phenylthiazol-5-yl)(4-(pyrimidin-2-yl)piperazin-1-yl)methanone) and antagonists (LP-471756 4-cyclohexyl-N-(o-tolyl)benzenesulfonamide and LP-114958 3-benzyl-N,5-dicyclohexyl-3H-[1,2,3]triazolo[4,5-d]pyrimidin-7-amine) for GPR139 (Hu et al., 2009). More recently, Wang et al identified five small molecule antagonists representing four different scaffolds (Wang et al., 2015). All of these compounds showed reasonable potency but little to no selectivity data was reported. While preparing this manuscript, Isberg and colleagues disclosed a pharmacophore model based on known surrogate GPR139 agonists to propose L-tryptophan (L-Trp) and L-phenylalanine (L-Phe) as putative endogenous ligands for GPR139 (Isberg et al., 2014).

The goal of the present study was to identify the physiologic ligand for GPR139. We measured GPR139 receptor activity in recombinant cells following treatment with various amino acids and orphan ligands. GPR139 activity in recombinant systems was measured using guanosine 5'-O-(3-[^{35}S]thio)-triphosphate ([^{35}S]GTPγS) binding, calcium mobilization and extracellular signal-regulated kinases (ERK) phosphorylation. Chromatography of rat serum, rat brain and human serum extracts was used to confirm the identity of the natural ligands. A high throughput screen was run to identify novel tool compounds to study GPR139 function. We applied RNA sequencing to study the expression of GPR139 in human and rat central nervous

systems. The distribution of GPR139 was then examined in greater detail in the mouse brain using an antibody specific for GPR139 and β-galactosidase as a marker for GPR139 expressing cells in brains from GPR139-null, lacZ knock-in mice. Lastly, a selective small molecule agonist JNJ-63533054 ([(S)-3-chloro-N-(2-oxo-2-((1-phenylethyl)amino)ethyl) benzamide]) and its less active enantiomer JNJ-63770044, ((R)-3-chloro-N-(2-oxo-2-((1-phenylethyl)amino)ethyl)benzamide), were tested for their effects on spontaneous locomotor activity in rats.

Materials and Methods

All animal procedures performed in this study were done in accordance with the Guide for the Care and Use of Laboratory Animals adopted by the US National Institutes of Health (NIH Publication no. 80-23 revised 1996) and the guidelines of the Institutional Animal Care and Use Committee.

Compounds:

All L-amino acids, D-tryptophan, 1-methy-L-tryptophan, 1-methy-D-tryptophan D-phenylalanine, amphetamine, trace amines, and biogenic amines were purchased from Sigma-Aldrich (Louisiana, MA). Other Phe and Trp derivatives were purchased from PepTech Corporation (Bedford, MA). JNJ-63533054 and JNJ-63770044 were synthesized at Janssen Research & Development, LLC as described in Dvorak et al. (Dvorak et al., 2015). (S)-3-bromo-5-chloro-N-(2-oxo-2-((1-phenylethyl)amino)ethyl)benzamide was utilized to prepare [^{3}H]JNJ-63533054 (24.7 Ci/mmol) via reduction of the bromide with tritium through a contract with Moravek Biochemicals (Brea, CA). The radiochemical purity of [^{3}H]JNJ-63533054 was determined to be 99.1% by high performance liquid chromatography (HPLC) analysis with radioactive flow detection. TC-O9311 (3,5-Dimethoxybenzoic acid 2-[(1-naphthalenylamino)carbonyl]hydrazide) was purchased from Tocris Bioscience (Bristol, United Kingdom). [^{35}S]-GTPγS (1250 Ci/mmol) was purchased from Perkin Elmer (Waltham, MA).

Molecular cloning of GPR139 from different species:

GPR139 from human, monkey, dog, mouse, rat, chicken, turtle and frog were cloned from respective brain cDNAs. A human GPR139 gene fragment was identified by blast (tblastn)

8

search of the human genomic sequence using human somatostatin 4 receptor as the template. The

5' end and 3'end of the human GPR139 were identified by rapid amplification of cDNA end

(RACE) using the human fetal brain cDNA as the template. The 5' and 3' ends, and the genomic

sequences of human GPR139 were used to assemble the full length coding region. The DNA

coding regions for GPR139 from other species were identified using the predicted human

GPR139 protein sequence to blast search (tblastn) the genomic sequences from respective

species. To clone the GPR139 cDNAs for recombinant expression, specific primers were used to

amplify the GPR139 coding regions from these species using the respective brain cDNAs as the

templates. Primers for human (forward: 5' ACG TCA GAA TTC GCC ACC ATG GAG CAC

ACG CAC GCC CAC CT 3'; reverse: 5' ATG TCA GCG GCC GCT CAC GGG GAT ACT

TTT ATA GGT TTT CCA TTT TTG TCA TAC TG 3'), monkey (forward: 5' ACG TCA GGT

ACC GCC ACC ATG GAG CAC ACG CAC GCC CAC CTC GCA GCC AAC A 3' ; reverse:

5' ATG TCA GCG GCC GCT CAC GGG GAT ACT TTT ATA GGT TTT CCA TTT TTG

TCA TAC TGG TAC 3'), dog (forward: 5'GTC TCA GGA TCC GCC ACC ATG GAG CAC

ACG CAC GCC CAC CTC GCC GCC 3'; reverse: 5' CTA CTA CTA CTA GCG GCC GCT

CAC GGG GAT ACT TTT ATA GGT TTT CCA TT 3'), mouse (forward: 5' ACT AGA GAA

TTC GCC ACC ATG GAG CAC ACG CAC GCC CAC CTC 3'; reverse: 5' ACT AGA GCG

GCC GCT CAC GGG GAT ACT TTT ATA GGC TTT CCA TG 3'), rat (forward: 5' ACT

AGA GAA TTC GCC ACC ATG GAG CAC ACG CAC GCC CAC CTC GCT GCG AAT AG

3'; reverse: 5' ACT AGA GCG GCC GCT CAC GGG GAT ACT TTT ATA GGC TTC CCA

TGT TTG TCA TAC TG 3'), chicken (forward: 5' ACG TCA GAA TTC GCC ACC ATG GAG

CAC AAC CAC CTC CAC CTC CAC AA 3'; reverse: 5' ACG TCA GCG GCC GCT CAT

9

GGT GAT ATT TTT ATA GGT TTT CCA TTC TTA TCA TAC TGG TAA 3'), turtle (forward:

5' ATC GTC GAA TTC GCC ACC ATG GAG TAC AAC CAC ATC CAC GTC CAC AAC 3';

reverse: 5' GAT GAG GCG GCC GCT CAT GGT GAT ATT TTT ATA GGT TTT CCA TTT

TTA TCA TAC TGG TAA ACA AGC 3') and frog (forward: 5' ACG TCA GAA TTC GCC

ACC ATG GAG CAC AAT CAC ATC TAC AAC ACT TCT 3'; reverse: 5' ACG TCA GCG

GCC GCT CAC GGG GAT ATT TTT AAT GGC TTC CCA TT 3') were designed according to

GPR139 coding regions from respective species. The PCR amplified cDNAs were then cloned

into the mammalian expression vector pCI-neo (Promega, Madison WI), and the inserts were

sequenced (Eton Biosciences, San Diego, CA) to verify identities. GPR139 DNA sequences

from these species were submitted to GenBank with accession numbers as follows: Human:

KR081941; Monkey: KR081942; Dog: KR081943; Mouse: KR081944; Rat: KR081945;

Chicken: KR081946; Turtle: KR081947; Frog: KR081948.

Luciferase reporter assay:

pSRE-Luc (Cat#219079), part of the PathDetect cis-reporting system, luciferase reporter

plasmid was obtained from Agilent Technologies (Santa Clara, CA). Parental human embryonic

293 cells (HEK293) were grown at 37^oC with 5% CO_2 in Dulbecco's Modified Eagle Medium

(DMEM/F12), no phenol red, containing 10% fetal bovine serum (FBS), 1X penicillin /

streptomycin, and 1 mM sodium pyruvate (Life Technologies). GPR139 expression plasmid was

transiently co-transfected with pSRE-Luc into HEK293 cells using Fugene HD (Promega,

Madison, WI) in 96-well white opaque plates. HEK293 cells transfected with GPR139 were

grown in custom made DMEM/F12 containing 10% FBS, 1X penicillin / streptomycin, 1 mM

sodium pyruvate and reduced Phe (30 μM) and Trp (10 μM). Two days post-transfection,

10

culture media was aspirated and cells were lysed with 1X cell culture lysis buffer contained in the luciferase assay kit (Promega). GPR139 induced luciferase activity was detected by addition of a chemiluminescent reagent (Promega). Chemiluminescence was read on the Envision (Perkin Elmer). Cells co-transfected with pCIneo and SRE-Luc were used as the control. Results were plotted using GraphPad Prism software version 6.02 (San Diego, CA). To determine whether differences were significant between cells transfected with GPR139 and control cells, an unpaired t-test was performed using GraphPad Prism software.

[^{35}S]GTPγS binding assay:

COS7 cells were grown at 37°C with 5% CO_2 in DMEM media (Corning, Corning, NY) containing 10% FBS, 1X penicillin / streptomycin, 1 mM sodium pyruvate, and 20 mM HEPES (4-(2-hydroxyethyl)-1-piperazineethanesulfonic acid). On the day of transfection, COS7 cells were plated to a density of 1.5 x 10^7 cells into 15 cm dishes and allowed to settle in the incubator for 3 h. COS7 cells were transiently co-transfected (Lipofectamine, Life Technologies, Grand Island, NY) with 20 µg total DNA of human GPR139 in pCIneo expression plasmid and a chimeric G-protein, G_{o2-q} (Genbank accession No: KR081949), expressed in pcDNA3.1/Zeo, at a ratio of 2:1, respectively. Two days post-transfection, cells were harvested in cold phosphate buffer saline (PBS) containing 10 mM ethylenediaminetetraacetic acid (EDTA). The cells were spun down at 5000 x g at 4°C and the pellets were frozen at -80°C. Membranes were prepared from frozen cell pellets and [^{35}S]-GTPγS binding assays were then performed as previously described (Liu et al., 2003). Crude membranes were prepared by homogenizing cell pellets in 50 mM Tris-HCl, pH 7.4, 5 mM EDTA followed by a 10 min centrifugation at 1000 revolutions per min (rpm) at 4°C. The supernatants were centrifuged for 30 min at 4°C at 15,000 rpm. The

pellets containing the crude cell membranes were homogenized in binding buffer (50 mM Tris-HCl, pH 7.4, 100 mM NaCl, 10 mM $MgCl_2$, 1 mM EDTA) and aliquoted in 96-well v-shaped plates (100 µl/well). The ligands (50 µl/well) were added to the cell membranes at room temperature and incubated for 20 min followed by addition of [^{35}S]GTPγS (0.1 µCi/well) and incubation for one hour at room temperature. The assay was terminated by filtration through GF/C filter plates (Perkin Elmer) and Microscint-40 (50 µl) was added to each well. Count rates were measured with a Topcount scintillation counter (Perkin Elmer). Cells co-transfected with pCIneo and Go2-q were used as negative controls. Results were analyzed using GraphPad prism software. To determine whether differences were significant between cells transfected with GPR139 and control cells upon stimulation with amino acids, an unpaired t-test was performed using GraphPad Prism software. A non-linear regression was used to determine the agonist EC_{50} values (concentration of the agonist that produced the half-maximal response). For the amino acid screen [^{35}S]GTPγS activity measured upon buffer incubation was arbitrarily set at 100 to normalize the data across experiments ([^{35}S]GTPγS activities stimulated by amino acids were expressed as a ratio vs the buffer).

ERK Phosphorylation assay:

Human GPR139 was cloned into pcDNA4/TO (Life Technologies, Grand Island, NY), part of the T-Rex inducible system. Expression in pcDNA4/TO was under the control of two tetracycline operator sites. Co-transfection with pcDNA6/TR (Life Technologies), which encoded the tetracycline repressor protein, turned off the expression of GPR139. Addition of tetracycline or doxycycline, a tetracycline analog, induced the expression of GPR139. An

inducible stable cell line expressing human GPR139 was made by co-transfecting GPR139-pcDNA4/TO expression plasmid and pcDNA6/TR into SK-N-MC cells, followed by selection with both zeocin and blasticidin. SK-N-MC cells stably expressing human GPR139 or SK-N-MC control cells were induced with doxycycline overnight in F12K media containing 10% tetracycline-free FBS, 1X penicillin / streptomycin (50 units penicillin, 50 µg streptomycin per ml), 1X non-essential amino acids (Life Technology, catalogue #11140-OSD) and 1 mM sodium pyruvate. Cells were washed with Hank's Balanced Salt Solution (HBSS) and incubated in HBSS for 2 h to remove Phe and Trp from the cell environment. Cells were then stimulated for 15 min with either 3 mM Phe, 3 mM Trp, or buffer alone. The cells were washed with ice cold PBS and lysed with 50 mM HEPES (pH 7.4) 150 mM sucrose, 80 mM β-glycerophosphate, 10 mM sodium fluoride, 10 mM pyrophosphate, 2 mM sodium orthovanadate, 2 mM EDTA, 1 % Triton X-100, 0.1% sodium dodecyl sulfate (SDS), 10 µg/ml aprotinin, 10 µg/ml leupeptin, and 1 mM phenylmethanesulfonylfluoride (PMSF). Samples were centrifuged at 12,000 rpm for 10 min at 4°C and the clear supernatants were run on a SDS-polyacrylamide gel electrophoresis (PAGE), transferred to polyvinylidene difluoride (PVDF) membrane and blotted first with anti-Phospho-ERK antibody (Cell Signaling Technology, Danvers, MA), stripped, and then blotted with anti-total ERK antibody (Cell Signaling Technology).

Calcium mobilization assay:

HEK293 cells stably or transiently transfected with GPR139 (human, rat and mouse) were grown to confluency in F-12K culture media (Corning) containing 10% FBS, 1X penicillin / streptomycin, 1X sodium pyruvate, 20 mM HEPES and 600 µg/ml G418. Cells were detached with 0.25 % trypsin/2.25 mM EDTA and re-suspended in plating media F-12K (Corning)

containing 10 % charcoal-treated FBS, 1X penicillin / streptomycin, 1X sodium pyruvate, 20 mM HEPES, and 600 μg/ml G418. Cells were seeded at 50 μl/well (50,000 cells/well) in poly-D-Lysine coated, black-walled, clear bottom 96-well tissue culture plates and incubated overnight at 37°C, 5% CO_2. On the day of the assay, cells were loaded with 2X BD calcium loading dye (Becton Dickinson, Franklin Lakes, NJ) solution at 50 μl/well and incubated at 37°C, 5% CO2 for 45 min. Compound dilutions were prepared in HBSS from 10 mM dimethyl sulfoxide (DMSO) stocks while Phe and Trp dilutions were prepared from 30 mM HBSS stocks. Compound, L-Phe and L-Trp additions (20 μl) were done on the Fluorometric Imaging Plate Reader (FLIPR) Tetra (Molecular Devices, Sunnyvale, CA) and changes in fluorescence which reflect calcium mobilization were monitored at 1-sec intervals for 90 sec followed by 3-sec intervals for 60 sec (excitation wavelength = 470-495 nm, emission wavelength = 515-575 nm). Data were exported as the difference between maximum and minimum fluorescence observed for each well. Results were calculated using non-linear regression to determine agonist EC_{50} values (Graphpad Prism software). E_{max} values are the percentage of the response elicited by the compound compared to 3 mM L-Trp.

The calcium mobilization assay in HEK293 cells transiently transfected with human GPR139 was also used to screen 140 Phe and Trp derivatives (PepTech Corporation) at 300 μM. The compounds showing greater or equal response to 300 μM L-Trp were then run at 4 concentrations with the highest concentration at 300 μM (two data points for each concentration). Results were calculated using non-linear regression to determine agonist EC_{50} values (Graphpad Prism software). E_{max} values were expressed as the percentage of the response elicited by the compound at 300 μM compared to 3 mM L-Trp.

14

Extraction of sera and tissues and identification of ligands for GPR139:

Human and rat sera were purchased from International Blood Bank Inc. (Memphis, TN) and Innovative Research, Inc. (Novi, MI), respectively. Extractions were prepared from sera or freshly dissected adult rat brains (male, Sprague Dawley, Harlan Laboratories, Livermore, CA) using ice cold ethanol/HCl (75% ethanol/ 25% 0.8 M HCl) at a sample to solvent ratio of 1:8. Extracts were centrifuged at 10,000 x g for 20 min at 4° C, and the clear supernatants were collected. The ethanol in the samples was evaporated under reduced pressure. The samples were then extracted using chloroform, and both phases were collected and dried. Samples were dissolved in mobile phase A (see below), filtered using 0.2 μm syringe filters and then fractionated with a Shimadzu prep HPLC consisting of two LC-8A pumps, a SIL-10AP auto injector, a SCL-10Avp system controller, and LCMS Solution software version 3. Column = Allure Organic Acid, 250 x 21 mm, 5 μm (Restek, Bellfonte, PA), room temperature; injection volume = 4 ml; mobile phases A = water with 1 mM HCl, pH~3, B = acetonitrile; flow rate = 25.5 ml/min; gradient = 0.01-1 min, 2% B; 1-12 min, ramp to 40% B; 12-15 min, hold at 40% B; 15-16 min, ramp to 90% B; 16-17 min, ramp down to 2% B; 17-24 min, hold at 2% B. Fractions were collected at 2 tubes/min with an ISCO Foxy200 fraction collector (Teledyne ISCO, Lincoln, NE) set to "collect by time" mode. Fractions were then tested for human GPR139 activation using [^{35}S]GTPγS binding assay (COS7 cells co-transfected with human GPR139 and chimeric G-protein G_{o2-q}). Cells membranes without GPR139 expression were used as negative controls. [^{35}S]GTPγS activity measured upon buffer (50 mM Tris-HCl, pH 7.5) incubation was arbitrarily set at 100 to normalize the data across experiments. [^{35}S]GTPγS activation by 3 mM L-Trp or 3 mM L-Phe were used as positive controls.

Radioligand binding assay:

Radioligand binding assays used human GPR139 expressed by clonal, inducible Chinese Hamster Ovary (CHO) cells. The human GPR139 cDNA was cloned into pcDNA4/TO (Invitrogen, Carlsbad, CA), which was then transfected into CHO-TRex cells (Invitrogen) by electroporation. After selection in complete medium (DM:F12 with 10% tetracycline-free fetal bovine serum (Omega Scientific, Tarzana CA), 50 iµ/ml pennicillin/50 µg/ml streptomycin, and 2 mM glutamine) with 2 µg/ml zeocin, the cells were cloned by limiting dilution. For testing, expression of GPR139 was induced for 20-24 hours with 1 µg/ml doxycycline. The cells were then removed from the plates with DPBS containing 5 mM EDTA, centrifuged at 500 x g for 3 min, then the fluid was aspirated away and the cell pellets were stored at -80°C. Pellets from T-Rex CHO cells expressing human GPR139 were homogenized in TE buffer (50 mM Tris HCl, pH 7.4, 5 mM EDTA) and spun down at 1000 rpm for 5 min at 4°C. Supernatant was collected and re-centrifuged at 15,000 rpm for 30 min at 4° C. The pellet was re-homogenized in TE buffer and incubated in a 96-well microtiter plate with eight concentrations of [^{3}H]JNJ-63533054 (specific activity 24.7 Ci/mmol) ranging from 0.41 nM to 600 nM for 60 min at room temperature (total volume 200 µL). The binding reaction was terminated by filtration through GF/C filterplates (FilterMate Harvester, Perkin Elmer) pre-treated with 0.1% polyethyleneimine followed by washes with cold TE buffer. Filterplates were dried in a 60° C oven for 30 min followed by addition of scintillation fluid. One hour later, bound radioactivity was counted on a Topcount NTX scintillation counter (Perkin Elmer). Non-specific binding was determined with 10 µM of TC-O9311. For inhibition of radioligand binding (10 nM [^{3}H]JNJ-63533054), compounds were added to the cell membrane (10 µg protein for human GPR139 and 30 µg

protein for rat GPR139) at seven concentrations ranging from 0.64 to 10,000 nM and L-Phe or L-Trp concentrations ranging from 0.19 to 3000 μM. Ligand concentration binding isotherms were also performed on membranes from HEK293 cells transiently transfected with rat or mouse GPR139. To determine whether differences were significant between total binding and non-specific binding, an unpaired t-test was performed using GraphPad Prism software. Ligand concentration binding isotherms and sigmoidal inhibition curves were generated and fitted using nonlinear regression analysis (GraphPad Prism software). The B_{max} and apparent K_d values of the radioligands and pIC_{50} of the inhibitor were free parameters for the curve fitting. Apparent K_i values were calculated as $K_i = IC_{50}/(1 + C/K_d)$, where C is concentration of the radioligand and $pK_i = -\log K_i$. Final protein content was assayed according to bicinchoninic acid protein assay kit protocol (Pierce, Rockford, IL).

Generation of GPR139 antibodies:

GPR139 antisera were made by immunizing rabbits with the peptide MEHTHAHLAANSSACGLG, which is the N-terminal of mouse GPR139 (Eton Biosciences). Immunized sera were tested by enzyme-linked immunosorbent assay using COS7 cells expressing mouse GPR139. Mock transfected COS7 cells served as control. Sera with high titer and high specificity were then affinity purified using the biotinylated antigens MEHTHAHLAANSSACGLG-gggg-K-biotin. Briefly, the biotinylated peptide (1 mg) was dissolved in 2 ml of 100 mM Tris-HCl,150 mM NaCl, pH 7.5 and then bound to 2 ml High Capacity NeutrAvidin Agarose and poured into a column (Thermo Scientific, Waltham, MA). The column was washed with 3 column volumes of alternating buffers of 100 mM Tris-HCl,150 mM NaCl pH 7.5 followed by 100 mM Gly-HCl, pH 2.8. Anti-GPR139 serum was then loaded

to the column, washed extensively using 100 mM Tris-HCl,150 mM NaCl, pH 7.5 and then eluted with 100 mM Gly-HCl, pH 2.8. The eluted antibodies were immediately neutralized using 1 M Tris-HCl, pH 8.0 and the antibody concentration was measured using an ultraviolet spectrometer. The purified antibodies were verified for specificity using recombinant cells expressing human, mouse and rat GPR139 for immunohistochemistry studies.

RNA sequencing:

Human RNA sequencing raw data of adult non-tumor tissue samples were obtained from The Genotype-Tissue Expression (GTEx) project (GTExConsortium., 2013) version 4 release. Additional human tissue samples from individual donors and rat pooled tissue samples ($\geq$ 4 Sprague-Dawley rats, 10 week old, Harlan Laboratories) were sequenced by BGI Americas (Cambridge, MA) with the Illumina HiSeq (San Diego, CA) platform using the GTEx protocols. All RNA sequencing data were processed using ArrayServer (Omicsoft, Cary, NC). Human sequences were mapped onto genome assembly GRCh37 and rat onto Rnor_5.0. Ensembl release 75 gene models were applied to represent genes in human and rat genomes. Fragments per kilobase per million mapped fragments (FPKM) were calculated to determine gene expression in each sample and to normalize across samples (Mortazavi et al., 2008). Samples failing raw data and mapping quality control, or having low consistency with other samples of the same tissue type were removed from the final data calculations.

Quantitative polymerase chain reaction studies:

Quantitative polymerase chain reaction (qPCR) was used to measure the expression of mouse and rat GPR139 mRNA expression in various tissues purchased from Clontech (Palo Alto,

CA). Primers for mouse (forward: 5' CGC TG CGA ATA GCT CGG CTT G 3'; reverse: 5' GTG GAT GGA GGA GAA CTC TAG A 3') and rat (forward: 5' TGA TCT TGT CAG GGA TCG GAG 3'; reverse: 5' CGC TGC GAA TAG CTC AGC TTG 3') GPR139 were used to amplify GPR139 cDNA. Primers for mouse (forward: 5' ACA ACG GCT CCG GCA TGT GCA 3'; reverse: 5' GTG TGG TGC CAG ATC TTC TCC A 3') and rat (forward: 5' CAA CAC AGT GCT GTC TGG TG 3'; reverse: 5' GAT CCA CAT CTG CTG GAA G 3') β-actin were used to amplify β-actin cDNA. A Perkin Elmer Light cycler was used for PCR reaction and data acquisition. The expression of GPR139 was normalized using the expression of β-actin.

Immunohistochemistry studies:

Wild-type C57Bl6 mice (10-12 weeks old, Charles River Laboratories, San Diego, CA) or GPR139 null, lacZ knockin mice (10-12 weeks, KOM repository, UC Davis, CA) were anesthetized by isofluorane and perfused transcardially using 4% paraformaldehyde in 0.1 M PBS solution. Brains were removed and post-fixed in 4% paraformaldehyde at room temperature for three hours followed by cryoprotection in 30% sucrose/PBS solution. Brains were embedded and frozen (Tissue-Tek, Sakura, Torrance, CA) and 20 μM coronal sections were cut and affixed to glass slides using a cryostat. For immunohistological staining, sections were washed three times in PBS and then blocked and permeabilized in a solution containing 10% normal goat serum, 1% bovine serum albumin, and 0.3% Triton X-100 in PBS for 2 hours at room temperature. Primary antibodies were diluted in PBS and incubated with sections overnight at 4° C. Sections were then washed in PBS at room temperature before a 1-hour incubation with fluorescently conjugated secondary antibodies. After washing in PBS, slides

19

were mounted using Vectashield Mounting Media (Vector Labs) and cover-slipped. Fluorescent images were acquired using a Zeiss LSM 700 confocal microscope. GPR139 antibody dilutions used for immunostaining ranged from 1-2 µg/ml. The β-galactosidase antibody was obtained through Abcam (AB9361) and used at a concentration of 2 µg/ml.

Extraction of plasma Trp and Phe from fasted or fed rats:

Plasma (150 µl) from Sprague-Dawley rats (Male 350-450g, Harlan Laboratories), freely fed (n =5) or fasted overnight (n = 6), was extracted with 400 µl of cold methanol, and the tube was put on a rocker at 4° C for one hour. After centrifugation at 14,000 x g for 20 min, the supernatants (150 µl from each sample) were collected into new Eppendorf tubes. Deuterated internal standards (Trp-d5 and Phe-d5) were added and solvent was evaporated with a Genevac. The samples were re-suspended in 150 µl mobile phase A (below), filtered through Durapore PVDF 0.22 µm spin filter (Millipore, Billerica, CA) and analyzed by liquid chromatography - mass spectrometry (LC/MS).

Quantification of plasma Trp and Phe:

Samples were analyzed on an Agilent 1290 HPLC coupled to qTOF 6500 mass spectrometer, with mobile phases: A = 98% water, 2% methanol, 0.1% formic acid; and B = acetonitrile, 0.1% formic acid; flow rate = 0.4 ml/min; injection volume = 10 µl. A Waters Atlantis T3 C18 column (150x2.1mm, 3u) was used at 40 ^{o}C to run the plasma samples. LC gradient: 0-2 min, 1% B; 2-8 min, 1-10% B; 8-13 min, 10-99%; 13-15 min, 99% B; 15-16 min, 99-1% B; 16-20 min, 1% B. Peaks were identified by exact mass and the retention times of

internal standards. Peak areas were calculated with Agilent's quantitative analysis software (ver. B.05.01) and converted to analyte concentrations/amounts using standard curves for Trp and Phe in the corresponding matrices.

Locomotor activity studies in rats:

Experiments were conducted in male Sprague-Dawley rats (350-450 g, Harlan Laboratories) housed individually under controlled conditions (12:12 light/dark schedule, temperature maintained at $22 \pm 2°C$, food and water *ad libitum*). Animals were chronically implanted with telemetric devices (Data Sciences International, St. Paul, MN) in the intraperitoneal cavity for the recording of locomotor activity within their individual home cage. Separate groups of rats were orally dosed at 2 h into the light phase with the GPR139 agonist JNJ-63533054 (3, 10 and 30 mg/kg, n=8 per dose), its less active enantiomer JNJ-63770044 (10 mg/kg, n=7) and L-Trp (200 mg/kg, n=7) or vehicle (0.5% hydroxypropyl methylcellulose in suspension) administered in the same animals receiving each dose.

For each experiment, signals were recorded on an IBM PC-compatible computer using Dataquest A.R.T. software (Data Sciences International, St. Paul, MN) for up to 10 h post dosing. Activity counts were analyzed into 1-min bins and averaged into 1-hour intervals for each animal. Results for all animals were then averaged by groups in defined time intervals. To determine whether differences at defined time intervals were significant between vehicle and compound administration in the same animal, a paired t-test was performed using GraphPad Prism software.

Results

Constitutive activity of GPR139 overexpressed in HEK293 cells.

In a luciferase reporter assay, HEK293 cells expressing human GPR139 show an approximately 8-times higher luciferase activity compared to HEK293 cells transfected with a control plasmid indicating that GPR139 has a high level of constitutive activity in this recombinant system (p<0.0001, **Figure 1**). This led us to hypothesize that the active ligand(s) for GPR139 may be present in the cell culture media.

GPR139 receptor activity in recombinant cells following treatment with amino acids.

A cell-free, $[^{35}S]$GTPγS binding assay using membranes from COS7 cells co-expressing human GPR139 and G_{o2}-q, a chimeric G-protein, was used to screen all 22 L-amino acids at a concentration of 3 mM. Both L-Trp and L-Phe stimulated $[^{35}S]$GTPγS binding in membranes obtained from cells expressing human GPR139 but not in membranes from control cells (L-Trp, p<0.0001; L-Phe, p=0.0007; **Figure 2A**). L-Trp and L-Phe failed to show stimulatory activity when tested against a panel of other GPCRs (data not shown). L-Trp and L-Phe stimulated $[^{35}S]$GTPγS binding in membranes from COS7 cells expressing human GPR139 in a concentration-dependent manner with EC_{50} values of 26 ± 4 μM and 31 ± 6 μM, respectively, (**Figure 2B**). L-Trp and L-Phe also stimulated a concentration-dependent calcium response in HEK293 cells transiently transfected with human GPR139 with EC_{50} values of 49 ± 11 μM and 60 ± 14 μM, respectively but not in control cells (**Figure 2C**). Similarly, L-Trp and L-Phe were tested for calcium mobilization in HEK293 cells stably expressing human GPR139 and showed

activity, although with higher EC_{50} values (287 ± 18 μM and 411 ± 70 μM, respectively) (data not shown).

Because many GPCRs signal downstream to the mitogen-activated protein kinase (MAPK)-ERK pathway, we tested whether L-Trp and L-Phe could stimulate GPR139-dependent ERK phosphorylation. Treatment of SK-N-MC cells expressing human GPR139 with 3 mM L-Trp or L-Phe led to increased ERK phosphorylation, whereas no stimulation was observed in control SK-N-MC cells (**Figure 2D**). Interestingly, basal ERK phosphorylation in human GPR139 expressing cells was higher than in control cells, possibly due to GPR139 activity caused by the presence of both L-Trp and L-Phe in the culture media.

Detecting endogenous GPR139 agonists from sera and brain extracts:

To investigate whether other endogenous ligands for GPR139 exist, we tested fractions from HPLC chromatographed human serum, rat serum and rat brain (**Figure 3**). Fractions 9, 10, 16 and 17 from human serum, rat serum and rat brain increased [^{35}S]GTPγS binding in membranes from COS7 cells expressing human GPR139 while no stimulatory activity was detected in control cell membranes. Phe could be detected in fractions 9 and 10 and Trp could be detected in fractions 16 and 17. 3 mM L-Phe and L-Trp were used as positive controls.

L-Trp and L-Phe concentrations in rat plasma:

For GPR139 to properly detect and respond to concentration changes of its endogenous ligands, their concentration would likely correspond to the EC_{50} values we observed earlier (**Figure 2B and 2C**). To test this, plasma from freely fed and fasted rats was collected and L-

Trp and L-Phe concentrations were measured. In freely fed rats, plasma concentrations were 188 ± 13 μM for L-Trp (n = 5) and 155 ± 11 μM for L-Phe (n = 5). Following fasting both L-Trp and L-Phe concentrations in the plasma decreased to 125 ± 6 μM (n = 6) and 121 ± 4 μM (ν = 6), respectively. These values fall within the dynamic range of GPR139 activity (30-300 μM) that we calculated from our *in vitro* recombinant system.

Amino acid sequence comparison of GPR139 from various species:

A comparison of amino acid sequence showed that GPR139 from various species are highly conserved (**Figure 4, Table 1**). The human receptor is identical to the monkey receptor, while it shares 99%, 94%, 92 %, 90%, and 88% identity with the dog, mouse/rat, chicken, turtle and frog receptors at the amino acid level, respectively. The mouse and rat receptors only differ by one residue and are identical in the transmembrane domain regions. The least conserved region appears at the N-terminus and the third extracellular loop (**Figure 4**). We tested the ability of L-Trp and L-Phe to stimulate a calcium response in cells transfected with GPR139 of various species. EC_{50} values were comparable to that of the human receptor (**Table 2).**

Screening of Trp and Phe derivatives for GPR139 activity:

D-Trp, D-Phe, 1-methyl-L-Trp, 1-methyl-D-Trp, and biogenic amines including trace amines were screened for human GPR139 activity using the calcium mobilization assay. Out of the 140 compounds screened, 66 compounds showed equal or greater activity than 300 μM L-Trp. These compounds are listed in **Table 3**. D-Trp and 1-methyl-Trp exhibited greater potency for GPR139 activation than L-Trp or L-Phe. Trace amines such as β-phenylethylamine, tryptamine, and amphetamine also activated GPR139 with potency similar to that of L-Trp and L-Phe.

However, octopamine, tyramine and the biogenic amines adrenaline, dopamine, histamine and serotonin did not activate GPR139 up to 0.3 mM. P-chlorophenylalanine (PCPA) was more potent than L-Trp and L-Phe, with an EC_{50} value of 24 ± 6 µM and 2.6 ± 0.3 µM for human and rat GPR139, respectively (**Supplementary Figure 1**). Interestingly, several compounds showed high E_{max} values (>150 %) (**Table 3**).

Identification of a selective high affinity GPR139 agonist:

A focused high throughput screen for GPR139 was completed from a library of 100,000 compounds (small molecules, diversity set) and agonist leads were identified (Dvorak et al., 2015). Structure activity relationship studies identified JNJ-63533054 (**Figure 5A**) as a potent and selective agonist. JNJ-63533054 specifically activated human GPR139 in the calcium mobilization ($EC_{50} = 16 \pm 6$ nM) and GTPγS binding ($EC_{50} = 17 \pm 4$ nM) assays. JNJ-63533054 also activated the rat and mouse GPR139 receptor with similar potency (rat $EC_{50} = 63 \pm 24$ nM, mouse $EC_{50} = 28 \pm 7$ nM). The corresponding enantiomer of JNJ-63533054 was also prepared (JNJ-63770044) and found to be ~ 100-fold less potent at human GPR139 ($EC_{50} = 1760 \pm 487$ nM). [3H]JNJ-63533054 (24.7 Ci/mmol) was used to develop a radioligand binding assay. Various buffers were tested to optimize the assay in pilot experiments. Addition of low concentration of NaCl and divalent ions did not shift the affinity of the tracer for GPR139 (data not shown). On membranes from T-Rex CHO cells expressing human GPR139, a high signal-to-noise ratio was observed (total vs non-specific binding p<0.0001), and no specific binding was detected in membranes from non-induced human GPR139 cells or control membranes from untransfected cells (**Figure 5B**). In a saturation study for human GPR139, a single population of high affinity binding sites for [3H] JNJ-63533054 was observed and the K_d (10 ± 3 nM) was in

agreement with the corresponding EC$_{50}$ (**Figure 5C**). The B$_{max}$ value was 26 ± 4 pmol/mg protein. Saturation studies for the rat GPR139 and mouse GPR139 yielded K$_d$ values within the same range (32 ± 13 nM and 23 ± 4 nM, respectively; B$_{max}$ = 8.5 ± 2.5pmol/mg protein and 6.2 ± 1.6pmol/mg protein, respectively). Using this radioligand, we further characterized the binding properties of L-Trp, L-Phe, JNJ-63533054, JNJ-63770044, amphetamine and PCPA (**Figure 5C**). β-PEA and tryptamine were also included and the affinity constants (K$_i$) are given in **Table 4**. Our results showed that both L-Trp and L-Phe competed for [^{3}H]JNJ-63533054 binding sites in T-REx CHO cells expressing human GPR139 with K$_i$ values of 738 ± 64 and 872 ± 7 μM, respectively. Amphetamine and PCPA also competed for [^{3}H]JNJ-63533054 binding. The affinity constants (K$_i$) measured for the human, rat and mouse GPR139 are listed in **Table 4**.

GPR139 expression in human and rat tissue:

RNA sequencing studies of human and rat tissues showed that GPR139 is almost exclusively expressed in brain tissue (**Figure 6**). Expression was also detected in pituitary, with much higher levels in rat compared to human samples. In human and rat brain, the highest levels were detected within the basal ganglia (caudate, putamen, nucleus accumbens), hypothalamus and thalamus. In rat, high levels were also detected in substantia nigra. Quantitative PCR data in mouse and rat brain confirmed the selective brain expression of GPR139 mRNA (**Supplemental Figure 2**).

To analyze expression and localization of GPR139 in mouse brain, a rabbit polyclonal antibody was generated using a portion of the N-terminus of mouse GPR139 as the antigen. The resulting antibody was specific for GPR139 as tested by Western blot and immunocytochemistry

in transfected cell lines (data not shown). The antibody also displayed species reactivity against mouse, rat and human GPR139 (**Supplemental Figure 3**). On mouse brain sections, this antibody displayed strong immunoreactivity in the medial habenula (**Figure 7A**). No immunoreactivity was detected in brain from GPR139 null, lacZ knock-in animals (**Figure 7B**). GPR139 null animals have the lacZ gene knocked into the GPR139 locus, resulting in the expression of beta-galactosidase (β-gal) under the control of the GPR139 promoter. We therefore used β-gal as a marker for GPR139 expressing cells. Immunostaining for β-gal revealed a large population of dorsal and ventral medial habenular neurons (**Figure 7C**). These GPR139-positive neurons appear to project axons via the fasiculus retroflexus to the interpeduncular nucleus, where β-gal immunoreactivity is detected (**Figure 7D, 7E**). Weak GPR139 expression is observed in the interpeduncular nucleus, suggesting that GPR139 may not have a presynaptic function. The other brain area found to display strong GPR139-positive immunoreactivity was the lateral septal nucleus. Staining of GPR139 in wild type mice or staining of β-gal in GPR139 lacZ knock-in mice revealed positive cell body and proximal fiber staining in one layer of the rostral lateral septum (**Figure 7F, 7G**).

Effect of GPR139 agonism, on locomotor activity in rats:

The effects on spontaneous locomotor activity of the GPR139 agonist JNJ-63533054 (3, 10 and 30 mg/kg), its less active enantiomer JNJ-63770044 (10 mg/kg) and L-Trp (200 mg/kg) were evaluated in rats following oral dosing at the beginning of the light/rest phase. The results are presented for the first hour after dosing based on the short-lasting effects observed (**Figure 8**). Compared to vehicle, the specific GPR139 agonist induced a dose-dependent reduction in locomotor activity in the first hour following the treatment that reached significance from the

dose of 10 mg/kg onwards (**Figure 8A**). In contrast, at the same dose of 10 mg/kg, its less active

enantiomer did not modify locomotor activity (**Figure 8B**). For comparison, L-Trp was tested in

the same experimental conditions and spontaneous locomotor activity was not affected at 200

mg/kg (**Figure 8C**).

Discussion

Here we demonstrated that the essential amino acids L-Trp and L-Phe activate GPR139, which is highly expressed in circumventricular regions of the central nervous system, namely the medial habenula and lateral septum regions. Based on our fractionation results, L-Trp and L-Phe are likely endogenous ligands for GPR139 in mammals, as they were the only detectable substances from tissues capable of activating GPR139, at least based on fractionation and assay conditions. While preparing this manuscript, Isberg and colleagues disclosed a pharmacophore model based on known surrogate GPR139 agonists to propose L-Trp and L-Phe as putative endogenous ligands for GPR139 (Isberg et al., 2014). Our experimental data are in agreement with that hypothesis and provide additional and independent biological and pharmacological evidence to support that L-Trp and L-Phe signal through GPR139.

L-Trp and L-Phe are endogenous ligands for GPR139:

In agreement with the literature (Matsuo et al., 2005) we observed that GPR139 displayed high levels of constitutive activity when recombinantly overexpressed in mammalian cell culture systems. We hypothesized that the active ligand for GPR139 may be present in the cell culture media and therefore devised a cell-free, [^{35}S]GTPγS binding assay using cell membranes from cells co-expressing GPR139 and a chimeric G-protein. Using this assay, we screened all 22 amino acids and demonstrated a robust stimulation of [^{35}S]GTPγS binding by L-Phe and L-Trp. Knowing that GPR139 is likely coupled with Gq (Matsuo et al., 2005), we designed a calcium assay with reduced amino acid concentrations in the culture media and observed robust calcium stimulation following L-Trp and L-Phe addition. We then demonstrated that GPR139 activation by L-Trp and L-Phe led to ERK phosphorylation, providing evidence in

a third functional assay that these two essential amino acids are capable of activating GPR139. In an attempt to identify other substances that may act as GPR139 endogenous ligands, we extracted rat, human sera and rat brain for peptides, small hydrophobic molecules, as well as small hydrophilic molecules, and looked for potential activators for GPR139 by [^{35}S]GTPγS binding assay which could tolerate relatively crude extracts. While we did not detect any active ingredient from peptide extracts or hydrophobic extracts, we observed two clear specific peaks of activity from human and rat sera and rat brain extract for hydrophilic small molecules. The active peaks had the same retention time as L-Trp and L-Phe, and mass spectrometry analysis confirmed the presence of L-Trp and L-Phe in the peaks. These results strongly suggest that L-Trp and L-Phe are the physiological ligands for GPR139, but we cannot rule out the existence of other potential ligands. Therefore, under the extraction methods employed and the assay conditions used, L-Trp and L-Phe, are the only substances detected capable of activating GPR139.

Our radioligand binding data using a high affinity agonist ligand [^{3}H]JNJ-63533054 indicates that both L-Trp and L-Phe directly interact with an agonist binding site on GPR139. There was a ~10-fold shift between affinity and potency for L-Trp and L-Phe. This shift was more pronounced for the human GPR139 compared to the mouse/rat receptors. This could be explained by the use of a stable cell line for the human radioligand binding and thus lower expression level compared to the transient transfection used for the rat and mouse GPR139. We performed subsequent *in vitro* functional experiments using a stable cell line and the potency values obtained were much closer to the affinity data and were in agreement with the results reported by Isberg and colleagues (Isberg et al., 2014). Unfortunately, the radioligand binding

assay was not suitable for native tissue despite testing various experimental parameters for ideal binding conditions. Radioligand autoradiography was also attempted in rodent septum and habenula but no specific binding was detected in any of the experimental condition tested (unpublished data). We speculate that GPR139 receptor density in native tissue might be too low for this agonist tracer. Future work will focus on developing a potent antagonist tracer and optimizing conditions for binding in brain tissue.

In general, ligands with low physiological concentrations require high affinity receptor interaction. On the other hand, ligands that are present in the body at high concentrations need only to have low affinity interactions with their receptors to mediate their regulatory functions in a dynamic range. The physiological concentrations of L-Trp and L-Phe measured in rat plasma in our experiment (50-200 μM) are in agreement with the literature (Fernstrom et al., 1979). Our results indicated that the plasma concentrations of L-Trp and L-Phe fluctuate under different physiological conditions within a pharmacological range capable of activating GPR139. The *in vitro* affinity and potency values of L-Trp and L-Phe for GPR139 are within the physiological concentration ranges of L-Trp and L-Phe. Thus, GPR139 is poised to sense the concentration changes of L-Trp and L-Phe under physiological conditions. Future experiments will address variation of Phe and Trp levels in brain tissue.

Endogenous ligand and receptor pairs are often conserved among species because the receptor evolves around its ligand, or *vice versa*. We cloned GPR139 from several mammals including human, monkey, dog, mouse and rat, as well as a few distant species including chicken, turtle, and frog. Sequence analysis indicates that the homology of the receptors across species is very high (greater than 80% across species). In addition, the receptors from those

distant species exhibited very similar pharmacological profiles in terms of their affinities to L-Trp and L-Phe. The high conservation of the receptor and ligands from distant species provides additional evidence that L-Trp and L-Phe are physiological ligands for GPR139. Interestingly, in 2013, Toda et al. disclosed surrogate ligands for GPR142 and referred to a "manuscript in preparation" describing that Trp is the endogenous ligand for GPR142 (Toda et al., 2013). In our hands, the effect of Trp on recombinant GPR142 is assay and species dependent (unpublished data). Our work on GPR142 is beyond the scope of the present publication.

PCPA activates GPR139:

As shown in **Table 3**, there are several other endogenous molecules that have higher affinity for GPR139 than L-Trp and L-Phe such as D-Trp, β-phenylethylamine and tryptamine. Octopamine, tyramine and all biogenic amines tested (adrenaline, dopamine, histamine, serotonin) did not activate GPR139. The trace amines β-phenylethylamine and tryptamine activated GPR139 with potency in the range of 20-50 μM which is at least 100 fold lower than their potency for the trace amine-associated receptors (Zucchi et al., 2006). To the best of our knowledge, none of these GPR139-activating substances exist in physiological concentrations sufficient to activate GPR139, except of L-Trp and L-Phe. In rat brains, the estimated concentration of trace amines are in the 0.1 to 100 nM range (Zucchi et al., 2006). It is, however, conceivable that there are unknown mechanisms that can store or concentrate these substances and release them locally on GPR139 expressing cells. We cannot rule out that hypothesis at this time.

Interestingly, PCPA which is an inhibitor for phenylalanine hydroxylase and tryptophan hydroxylase and is often used in studies for serotonin depletion (Koe and Weissman, 1966), also

activated GPR139. In the dose range used for serotonin depletion studies in rodents (100-300 mg/kg, intraperitoneal) plasma exposure of PCPA reached levels ~ 725 μM (Kramer et al., 2010) which is well above the EC_{50} for rat GPR139 activation (2.6 μM) (**Supplementary Figure 1**). It will be interesting to evaluate the behavioral effect of PCPA in GPR139 knockout mice and to determine whether any previous interpretations of depletion studies needs to be revised in the context of GPR139 activation.

GPR139 expression and distribution in the brain and its implication for receptor functions:

Other groups have shown that in human and mouse tissue, GPR139 is predominantly expressed in the brain (Matsuo et al., 2005; Susens et al., 2006). Our RNA sequencing data largely confirmed and extended these findings and showed that the expression of GPR139 in both rat and human tissue is almost exclusive to the central nervous system, with the exception of expression observed in the pituitary. Using beta-galactosidase as a marker for GPR139 expressing cells in brains from GPR139 null, lacZ knock-in animals, we confirmed and extended the *in situ* hybridization results reported in the literature (Matsuo et al., 2005). GPR139 expressing neurons were found in regions of the brain close to ventricles, in the habenula and septum. In the habenula, GPR139-positive neurons project axons via the fasiculus retroflexus to the interpeduncular nucleus, where both GPR139 and β-gal immunoreactivity is detected. The expression of GPR139 in the medial habenula is interesting, as the mammalian habenula is involved in regulating the activities of serotonergic and dopaminergic neurons (Hikosaka, 2010; Proulx et al., 2014). In contrast to the lateral habenula, the medial habenula is relatively under-studied. It is a conserved region of the brain that has been considered as a part of the limbic

circuits involved in the regulation of mood and stress (Hsu et al., 2014; Morris et al., 1999; Proulx et al., 2014; Viswanath et al., 2014).

The other brain area found to display GPR139-positive immunoreactivity and GPR139 mRNA is the lateral septal nucleus. Positive cell body and proximal fiber staining were detected in one layer of the rostral lateral septum. Neurons from the lateral septum have been shown to modulate neuroendocrine and behavioral stress responses (Singewald et al., 2011). Experiments to further classify GPR139 expressing neurons will be informative to better understand the potential consequences of receptor activation. In addition, experiments using small molecule agonists and antagonists of GPR139, as well as GPR139 null mice will test whether receptor activation affects the function of these neurons in the habenula and septum, and leads to changes in behavior.

Administration of JNJ-63533054 in rats decreases locomotor activity:

The small molecule JNJ-63533054 was found to be devoid of any cross reactivity as judged by an external selectivity panel of 50 known GPCRs, ion channels, and transporters and it displayed suitable pharmacokinetic properties for *in vivo* studies (Dvorak et al., 2015). Information on the selectivity and pharmacokinetics of the GPR139 surrogate agonists previously published (TCO-9311 and LP-360924) are limited as compared to JNJ-63533054. TCO 9311 was found to be a P-glycoprotein substrate with very limited ability to cross the blood brain barrier (Shi et al., 2011). In contrast, JNJ-63533054 crosses the rat blood brain barrier after oral administration and achieves exposure in the micromolar range (Dvorak et al., 2015). Structurally, JNJ-63533054 possesses functional group elements that can be found in the reported hydrazinecarboxamide agonist (TCO-9311) (Shi et al., 2011) having two carbonyls in a

1,4 relationship, separated by two atoms and accompanied by a large flanking hydrophobic surface. It contains fewer hydrogen bond donors and acceptors than the hydrazinecarboxamide agonist and thus was found to have better physicochemical properties. Interestingly, JNJ-63533054 administration decreased spontaneous locomotor activity in rats. The specificity of this effect was corroborated by parallel evaluation of the less active enantiomer of JNJ-63533054 which achieved equal exposure in the brain (data not shown) but elicited no change in locomotor activity. Future work is needed to elucidate whether the mechanism behind this locomotor effect was mediated by GPR139 in the medial habenula. Although the literature is conflicting, some studies have shown that L-Trp administration can induce mild sedative effects (Fernstrom, 2012; Silber and Schmitt, 2010). In susceptible humans and in some animal models, reduced Trp and Phe intake has been shown to be depressogenic, whereas anecdotal reports of L-Trp and L-Phe loading are reported to have mood elevating effects (Silber and Schmitt, 2010). The effects of altered L-Trp and L-Phe levels on behavior have been hypothesized to be mediated by their downstream conversion to serotonin or dopamine. GPR139 could represent a mechanism to detect levels of the essential amino acids and signal to produce the appropriate response to changes in their concentrations. It remains to be determined whether L-Trp and/or L-Phe are stored and released like *bona fide* neurotransmitters or whether they act as sensors for the exterior milieu. In a preliminary experiment using *in vivo* microdialysis in rat brain, we did not observe any increase in L-Trp or L-Phe concentration upon potassium depolarization. The localization of GPR139 expressing neurons in circumventricular brain regions potentially places the receptor in the correct position for sensing L-Trp and L-Phe levels in circulating

cerebrospinal fluid. These lines of evidence suggest that GPR139 is a sensor for slower steady-state level changes in L-Trp and L-Phe concentration, rather than a neurotransmitter receptor.

Conclusions:

Our experimental results suggest that L-Trp and L-Phe are physiological ligands for GPR139 through which these substances may have biological and behavioral effects without relying on their conversion to biogenic amines. We hypothesize that GPR139 is a sensor to detect dynamic changes of L-Trp and L-Phe under physiological conditions and may thus provide the brain a mechanism to probe and react to metabolic changes.

Acknowledgment

We thank Dr. Caroline Lanigan for her advice on statistical analysis and Dr. Kevin Sharp and his staff for their assistance with *in vivo* work. We also thank Dr. de Lecea and Dr. Whittle for providing us with the GPR139 null, lacZ knockin mouse brains.

Authorship Contributions

Participated in research design: Changlu Liu, Christine Dugovic, Anthony Harrington, Jiejun Wu, Pascal Bonaventure, Timothy Lovenberg.

Conducted experiments: Changlu Liu, Grace Lee, Diane Nepomuceno, Chester Kuei, Victory Joseph, Jiejun Wu, William Eckert, Steven Sutton, Sujin Yu, Anthony Harrington.

Contributed new reagents or analytic tools: Curt Dvorak, Heather Coate, Nicholas Carruthers.

Performed data analysis: Changlu Liu, Grace Lee, Diane Nepomuceno, Chester Kuei, Victory Joseph, Xiang Yao, Lynn Yieh, Qingqin Li, Jiejun Wu, Christine Dugovic, Anthony Harrington, Pascal Bonaventure.

Wrote or contributed to the writing of the manuscript: Changlu Liu, Christine Dugovic, Jiejun Wu, Anthony Harrington, Pascal Bonaventure, Timothy Lovenberg.

ReferencesCivelli O, Reinscheid RK, Zhang Y, Wang Z, Fredriksson R and Schioth HB (2013) G protein-coupled receptor deorphanizations. *Annu Rev Pharmacol Toxicol* **53**:127-146.

Dvorak C, Coate H, Nepomuceno D, Wennerholm M, Kuei C, Lord B, Woody D, Bonaventure P, Liu C, Lovenberg T and Carruthers N (2015) Identification and SAR of glycine benzamides as potent agonists for the GPR139 receptor. *ACS Medicinal Chemistry Letters* in press.

Fernstrom JD (2012) Effects and Side Effects Associated with the Non-Nutritional Use of Tryptophan by Humans. *The Journal of Nutrition* **142**(12):2236S-2244S.

Fernstrom JD, Wurtman RJ, Hammarstrom-Wiklund B, Rand WM, Munro HN and Davidson CS (1979) Diurnal variations in plasma concentrations of tryptophan, tryosine, and other neutral amino acids: effect of dietary protein intake. *The American Journal of Clinical Nutrition* **32**(9):1912-1922.

Fredriksson R, Lagerstrom MC, Lundin LG and Schioth HB (2003) The G-protein-coupled receptors in the human genome form five main families. Phylogenetic analysis, paralogon groups, and fingerprints. *Mol Pharm* **63**(6):1256-1272.

Fredriksson R and Schiöth HB (2005) The Repertoire of G-Protein-Coupled-Receptors in Fully Sequenced Genomes. *Mol Pharm* **67**(5):1414-1425.

Gloriam DE, Schioth HB and Fredriksson R (2005) Nine new human Rhodopsin family G-protein coupled receptors: identification, sequence characterisation and evolutionary relationship. *Biochim Biophys Acta* 1722(3):235-246.

GTExConsortium. (2013) The Genotype-Tissue Expression (GTEx) project. *Nat Genet* **45**(6):580-585.

Heng BC, Aubel D and Fussenegger M (2013) An overview of the diverse roles of G-protein coupled receptors (GPCRs) in the pathophysiology of various human diseases. *Biotechnol Adv* **31**(8):1676-1694.

Hikosaka O (2010) The habenula: from stress evasion to value-based decision-making. *Nat Rev Neurosci* **11**(7):503-513.

Hsu YW, Wang SD, Wang S, Morton G, Zariwala HA, de la Iglesia HO and Turner EE (2014) Role of the dorsal medial habenula in the regulation of voluntary activity, motor function, hedonic state, and primary reinforcement. *J Neurosci* **34**(34):11366-11384.

Hu LA, Tang PM, Eslahi NK, Zhou T, Barbosa J and Liu Q (2009) Identification of surrogate agonists and antagonists for orphan G-protein-coupled receptor GPR139. *J Biomol Screen* **14**(7):789-797.

Isberg V, Andersen KB, Bisig C, Dietz GP, Brauner-Osborne H and Gloriam DE (2014) Computer-aided discovery of aromatic l-alpha-amino acids as agonists of the orphan G protein-coupled receptor GPR139. *J Chem Inf Model* **54**(6):1553-1557.

Koe BK and Weissman A (1966) p-Chlorophenylalanine: a specific depletor of brain serotonin. *J Pharmacol Exp Ther* **154**(3):499-516.

Kramer JA, ONeill E, Phillips ME, Bruce D, Smith T, Albright MM, Bellum S, Gopinathan S, Heydorn WE, Liu X, Nouraldeen A, Payne BJ, Read R, Vogel P, Yu X-Q and Wilson AGE (2010) Early Toxicology Signal Generation in the Mouse. *Toxicologic Pathology* **38**(3):452-471.

Liu C, Eriste E, Sutton S, Chen J, Roland B, Kuei C, Farmer N, Jarnvall H, Sillard R and Lovenberg TW (2003) Identification of Relaxin-3/INSL7 as an Endogenous Ligand for the Orphan G-protein-coupled Receptor GPCR135. *Journal of Biological Chemistry* **278**(50):50754-50764.

Lundstrom KH and Chiu ML (2005) *G Protein-Coupled Receptors in Drug Discovery*. CRC Taylor and Francis Group, London.

Matsuo A, Matsumoto S, Nagano M, Masumoto KH, Takasaki J, Matsumoto M, Kobori M, Katoh M and Shigeyoshi Y (2005) Molecular cloning and characterization of a novel Gq-coupled orphan receptor GPRg1 exclusively expressed in the central nervous system. *Biochem Biophys Res Commun* **331**(1):363-369.

Morris JS, Smith KA, Cowen PJ, Friston KJ and Dolan RJ (1999) Covariation of Activity in Habenula and Dorsal Raphé Nuclei Following Tryptophan Depletion. *NeuroImage* **10**(2):163-172.

Mortazavi A, Williams BA, McCue K, Schaeffer L and Wold B (2008) Mapping and quantifying mammalian transcriptomes by RNA-Seq. *Nat Methods* **5**(7):621-628.

Overington JP, Al-Lazikani B and Hopkins AL (2006) How many drug targets are there? *Nat Rev Drug Discov* **5**(12):993-996.

Proulx CD, Hikosaka O and Malinow R (2014) Reward processing by the lateral habenula in normal and depressive behaviors. *Nat Neurosci* **17**(9):1146-1152.

Shi F, Shen JK, Chen D, Fog K, Thirstrup K, Hentzer M, Karlsson JJ, Menon V, Jones KA, Smith KE and Smith G (2011) Discovery and SAR of a Series of Agonists at Orphan G Protein-Coupled Receptor 139. *ACS Med Chem Lett* **2**(4):303-306.

Silber BY and Schmitt JAJ (2010) Effects of tryptophan loading on human cognition, mood, and sleep. *Neuroscience & Biobehavioral Reviews* **34**(3):387-407.

Singewald GM, Rjabokon A, Singewald N and Ebner K (2011) The Modulatory Role of the Lateral Septum on Neuroendocrine and Behavioral Stress Responses. *Neuropsychopharmacology* **36**(4):793-804.

Susens U, Hermans-Borgmeyer I, Urny J and Schaller HC (2006) Characterisation and differential expression of two very closely related G-protein-coupled receptors, GPR139 and GPR142, in mouse tissue and during mouse development. *Neuropharmacology* **50**(4):512-520.

Toda N, Hao X, Ogawa Y, Oda K, Yu M, Fu Z, Chen Y, Kim Y, Lizarzaburu M, Lively S, Lawlis S, Murakoshi M, Nara F, Watanabe N, Reagan JD, Tian H, Fu A, Motani A, Liu Q, Lin YJ, Zhuang R, Xiong Y, Fan P, Medina J, Li L, Izumi M, Okuyama R and Shibuya S (2013) Potent and Orally Bioavailable GPR142 Agonists as Novel Insulin Secretagogues for the Treatment of Type 2 Diabetes. *ACS Med Chem Lett* **4**(8):790-794.

Viswanath H, Carter AQ, Baldwin PR, Molfese DL and Salas R (2014) The medial habenula: still neglected. *Front Hum Neurosci* **7**:931.

Wang J, Zhu L-y, Liu Q, Hentzer M, Smith GP and Wang M-w (2015) High-throughput screening of antagonists for the orphan G-protein coupled receptor GPR139. *Acta Pharmacol Sin* **36**(7):874-878.

Zucchi R, Chiellini G, Scanlan TS and Grandy DK (2006) Trace amine-associated receptors and their ligands. *British Journal of Pharmacology* **149**(8):967-978.

Footnotes

Changlu Liu and Pascal Bonaventure contributed equally to this work.

Reprint requests should be addressed to Pascal Bonaventure, 3210 Merryfield Row, CA92121

San Diego. Pbonave1@its.jnj.com. 858-784-3078.

Figure Legends

Figure 1:

Activity of GPR139 in recombinant cells.

Luciferase activity in HEK293 cells transiently co-transfected with human GPR139 and SRE-Luciferase reporter and in control cells. Results are presented as means ± S.D. (n = 3). ***p<0.001, unpaired t-test.

Figure 2:

Activation of GPR139 with L-Trp and L-Phe.

(**A**) [^{35}S]GTPγS binding activity following stimulation of all 22 L-amino acids at a concentration of 3 mM on membranes from COS7 cells transfected with human GPR139 (lower panel) or on control cells (upper panel). [^{35}S]GTPγS activity measured upon buffer incubation was arbitrarily set at 100. Results are presented as means ± S.D. (n = 3). ***p<0.001, unpaired t-test. (**B**) Concentration response of L-Trp and L-Phe [^{35}S]GTPγS binding in membranes from COS7 cells transfected with human GPR139 (right panel) and control cells (left panel). (C) Concentration response of L-Phe and L-Trp calcium mobilization in HEK293 cell transfected with human GPR139 (right panel) or control cells (left panel). Data shown in panels B and C are means ± S.D. (n = 2). (D) Western blot of ERK phosphorylation and total ERK following stimulation of buffer or 3 mM L-Trp and L-Phe in SK-N-MC cells expressing human GPR139 (top) or control cells (bottom) (n = 2).

Figure 3:

Detection of endogenous GPR139 ligands from human serum, rat serum, and rat brain extracts.

[^{35}S]GTPγS binding in membranes from COS7 cells transfected with human GPR139 (left panels) or control cells (right panels) following stimulation with fraction of HPLC chromatographed human serum, rat serum and rat brain extracts. 3 mM L-Trp and L-Phe positive control. [^{35}S]GTPγS activity measured upon buffer incubation was arbitrarily set at 100. Results are presented as means ± S.D. (n = 2).

Figure 4:

Amino acid sequences of GPR139 from various species.

Hydrophobic, hydrophilic, acidic, and basic residues are shown in red, green, blue and purple, respectively. "*****", "**:**", and "**.**" indicate residues that are identical, strongly, or weakly conserved among the species, respectively. Predicted transmembrane domain regions are underlined.

Figure 5:

Radioligand binding assay using [^{3}H]JNJ-63533054.

(**A**) Chemical structure of JNJ-63533054 [(S)-3-chloro-N-(2-oxo-2-((1-phenylethyl)amino)ethyl) benzamide]. (**B**) Total and nonspecific binding of [^{3}H]JNJ-63533054 on membranes from TRex CHO cells transfected with human GPR139 and control cells. (**C**) Concentration binding isotherm of [^{3}H]JNJ-63533054 on membranes from CHO-TRex cells transfected with human

GPR139. (**D**) Competition of [³H]JNJ-63533054 binding by JNJ-63533054, JNJ-63770044, L-Trp, L-Phe, amphetamine (AMP) and PCPA on membranes from TRex CHO cells transfected with human GPR139. Results are presented as means ± S.D. (n = 3). ***p<0.001, unpaired t-test.

Figure 6:

GPR139 gene expression in human and rat tissues by RNA sequencing.

RNA sequencing data showing GPR139 mRNA expression in (**A**) rat and (**B**) human tissues. FPKM: Fragments Per Kilobase per Million mapped fragments. Tissues are grouped by organ systems. Car: Cardiovascular, Dig: Digestive; End: Endocrine, Imm: Lymphatic, Int: Integumentary; Mus: Muscular, NerC: Central Nervous, Rep: Reproductive, Res: Respiratory, Uri: Urinary.

Figure 7:

Distribution of GPR139 in mouse brain. (**A**) GPR139 immunoreactivity in habenular axon fibers in wildtype mice. (**B**) Absence of GPR139 immunoreactivity in brain from GPR139 null, lacZ knock-in animals. (**C**) Immunostaining for β-gal revealed in habenular neurons (**D**) GPR139 immunoreactivity in interpeduncular nucleus (**E**) β-gal immunoreactivity in interpeduncluar nucleus (**F**) GPR139 immunoreactivity in the lateral septal nucleus (**G**) β-gal immunoreactivity in the rostral lateral septum. Scale bars in all panels equal 100 microns and insert scale bars in F and G are 50 microns.

Figure 8:

Effect of GPR139 agonism on spontaneous locomotor activity in rats.

Locomotor activity counts in the first hour after oral administration of (**A**) JNJ-63533054 (3, 10 and 30 mg/kg), (**B**) JNJ-63770044 (10 mg/kg) and (**C**) L-Trp (200 mg/kg). Values are means ± S.E.M. of 7-8 animals per compound. *$p < 0.05$, paired t-test.

Tables

Table 1:

Amino acid sequence identities (%) among GPR139 receptors from various species.

	Human	Monkey	Dog	Mouse	Rat	Chicken	Turtle	Frog
Human	100	100	99	94	94	92	90	88
Monkey		100	99	94	94	92	90	88
Dog			100	93	93	92	90	88
Mouse				100	99	89	88	86
Rat					100	89	88	86
Chicken						100	95	91
Turtle							100	91
Frog								100

Table 2:
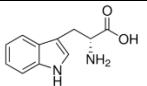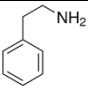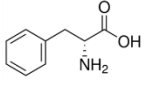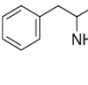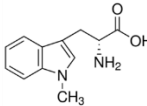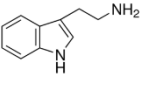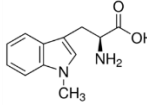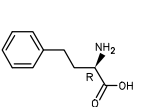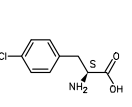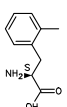
Agonist Potency (EC$_{50}$) of L-Phe and L-Trp at GPR139 from various species. Potency values were determined using a calcium mobilization assay in HEK293 cells transiently transfected with GPR139 cDNAs from respective species. EC$_{50}$ values (µM) are means ± S.D. (n = 2).

	Human EC$_{50}$ (µM)	Monkey EC$_{50}$ (µM)	Dog EC$_{50}$ (µM)	Mouse EC$_{50}$ (µM)	Rat EC$_{50}$ (µM)	Chicken EC$_{50}$ (µM)	Turtle EC$_{50}$ (µM)	Frog EC$_{50}$ (µM)
L-Trp	49 ± 11	55 ± 7	30 ± 5	54 ± 16	61 ± 13	33 ± 9	108 ± 18	99 ± 12
L-Phe	60 ± 14	68 ± 18	31 ± 8	56 ± 9	68 ± 21	47 ± 12	106 ± 21	116 ± 19

Table 3:
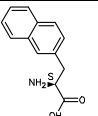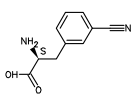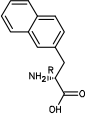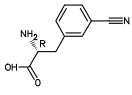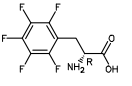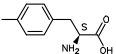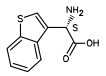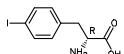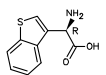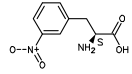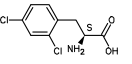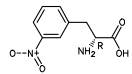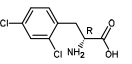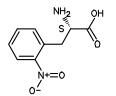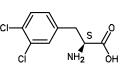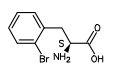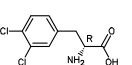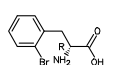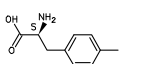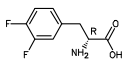
Agonist potency of L-Phe and L-Trp derivatives for human GPR139. Potency values were determined using a calcium mobilization assay in HEK293 cells transiently transfected with human GPR139. E_{max} values were expressed as the percentage of the response elicited by the compound at 300 μM compared to 3 mM L-Trp. ND, not determined because the concentration response curve did not reach saturation. Compounds were screened at 4 concentrations with two data points for each concentration.

Compound	Structure	EC_{50} μM	E_{max} %		Compound	Structure	EC_{50} μM	E_{max} %
D-Tryptophan		18	125		β-Phenethylamine		42	96
D-Phenylalanine		ND	56		Amphetamine		53	94
1-methyl-D-Trptophan		8	116		Tryptamine		16	102
1-methyl-L-Trptophan		13	103		(2R)-2-amino-4-phenyl-butanoic acid		ND	76
4Cl-L-Phenylalanine (PCPA)		24	156		2-methyl-L-phenylalanine		40	170
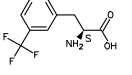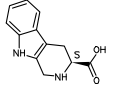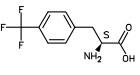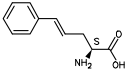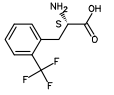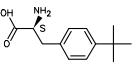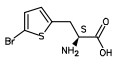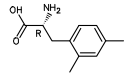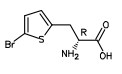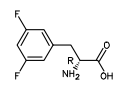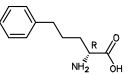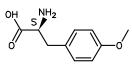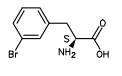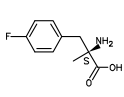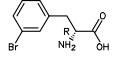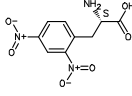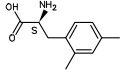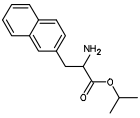
MOL#100412

4Cl-D-Phenylalanine		92	130		2-methyl-D-phenylalanine		ND	75
2F-L-Phenylalanine		ND	72		(2R)-2-amino-3-(4-nitrophenyl)propanoic acid		ND	44
3F-L-Phenylalanine		ND	93		3-methyl-L-phenylalanine		52	134
3F-D-Phenylalanine		ND	64		3-methyl-D-phenylalanine		87	115
4F-L-Phenylalanine		ND	63		(3R)-1,2,3,4-tetrahydroisoquinoline-3-carboxylic acid		37	167
4F-D-Phenylalanine		ND	58		3Cl-L-Phenylalanine		20	178
3Cl-D-Phenylalanine		44	161		4-methyl-D-phenylalanine		ND	57
4Br-L-Phenylalanine		12	172		(2S)-2-amino-3-(1-naphthyl)propanoic acid		5	175
4Br-D-Phenylalanine		47	75		(2S)-2-amino-3-(2-naphthyl)propanoic acid		5	162

51

Name	Structure				Name	Structure		
(2S)-2-amino-3-(2-naphthyl)propanoic acid		6	187		(2S)-2-amino-3-(3-cyanophenyl)propanoic acid		ND	35
(2R)-2-amino-3-(2-naphthyl)propanoic acid		16	152		(2R)-2-amino-3-(3-cyanophenyl)propanoic acid		ND	39
(2R)-2-amino-3-(2,3,4,5,6-pentafluorophenyl)propanoic acid		62	93		4,I-L-Phenylalanine		6	175
(2S)-2-amino-2-(benzothiophen-3-yl)acetic acid		ND	89		4,I-D-Phenylalanine		22	117
(2R)-2-amino-2-(benzothiophen-3-yl)acetic acid		ND	145		(2S)-2-amino-3-(3-nitrophenyl)propanoic acid		16	121
2,4,Cl-L-Phenylalanine		12	156		(2R)-2-amino-3-(3-nitrophenyl)propanoic acid		91	144
2,4,Cl-D-Phenylalanine		12	143		(2S)-2-amino-3-(2-nitrophenyl)propanoic acid		ND	96
3,4,Cl-L-Phenylalanine		3	198		2-Br-L-Phenylalanine		4	184
3,4,Cl-D-Phenylalanine		6	104		2-Br-D-Phenylalanine		ND	83
4-methyl-L-phenylalanine		22	192		3,4,F-D-Phenylalanine		100	72

Name	Structure			Name	Structure		
(2S)-2-amino-3-[3-(trifluoromethyl)phenyl]propanoic acid		3	95	(3S)-2,3,4,9-tetrahydro-1H-pyrido[3,4-b]indole-3-carboxylic acid		48	116
(2S)-2-amino-3-[4-(trifluoromethyl)phenyl]propanoic acid		5	114	(E,2S)-2-amino-5-phenyl-pent-4-enoic acid		ND	61
(2S)-2-amino-3-[2-(trifluoromethyl)phenyl]propanoic acid		38	98	(2S)-2-amino-3-(4-tert-butylphenyl)propanoic acid		ND	60
(2S)-2-amino-3-(5-bromo-2-thienyl)propanoic acid		49	186	2,4, dimethyl-D-Phenylalanine		21	118
(2R)-2-amino-3-(5-bromo-2-thienyl)propanoic acid		37	173	3,5,difluoro-D-Phenylalanine		ND	69
(2R)-2-amino-5-phenyl-pentanoic acid		58	146	(2S)-2-amino-3-(4-methoxyphenyl)propanoic acid		ND	71
3Br-L-Phenylalanine		10	193	(2S)-2-amino-3-(4-fluorophenyl)-2-methyl-propanoic acid		ND	61
3Br-D-Phenylalanine		18	182	(2S)-2-amino-3-(2,4-dinitrophenyl)propanoic acid		ND	73
2,4, dimethyl-L-Phenylalanine		23	128	isopropyl 2-amino-3-(2-naphthyl)propanoate		56	156

Table 4:

Inhibition equilibrium constants (K_i) of compounds for inhibition of [^{3}H]JNJ-63770044 binding

to membranes of cells expressing recombinant human, rat or mouse GPR139. K_i values (μM)

are means ± S.D. (n = 3).

	Human GPR139 T-Rex CHO K_i values (μM)	Rat GPR139 HEK-293 K_i values (μM)	Mouse GPR139 HEK-293 K_i values (μM)
L-Trp	738 ± 64	187 ± 30	242 ± 83
L-Phe	872 ± 7	117 ± 9	172 ± 52
JNJ-63533054	0.024 ± 0.003	0.075 ± 0.025	0.054 ± 0.012
JNJ-63770044	3.2 ± 0.7	3.5 ± 0.6	3.7 ± 1.0
Amphetamine	322 ± 146	62 ± 12	71 ± 10
PCPA	104 ± 45	12 ± 2	16 ± 3
β-PEA	459 ± 268	114 ± 15	107 ± 24
Tryptamine	337 ± 179	115 ± 13	105 ± 19
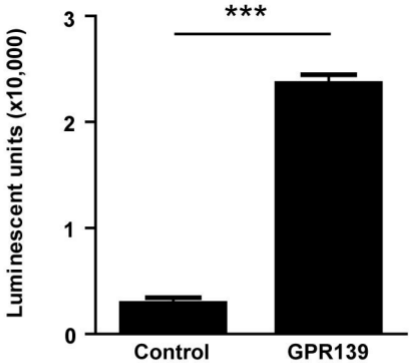
Figure 1

Figure 2

Figure 3

Figure 4

Figure 5

A RAT

B HUMAN

Figure 6

Figure 7

Figure 8